THE JOURNAL OF PHYSICAL CHEMISTRY B

Article

pubs.acs.org/JPCB

The Influence of Cholesterol on Fast Dynamics Inside of Vesicle and Planar Phospholipid Bilayers Measured with 2D IR Spectroscopy

Oksana Kel, Amr Tamimi, and Michael D. Fayer*

Department of Chemistry, Stanford University, Stanford, California 94305-5080, United States

ABSTRACT: Phospholipid bilayers are frequently used as models for cell membranes. Here the influence of cholesterol on the structural dynamics in the interior of 1,2-dilauroyl-*sn*-glycero-3-phosphocholine (dilauroylphosphatidylcholine, DLPC) vesicles and DLPC planar bilayers are investigated as a function of cholesterol concentration. 2D IR vibrational echo spectroscopy was performed on the antisymmetric CO stretch of the vibrational probe molecule tungsten hexacarbonyl, which is located in the interior alkyl regions of the bilayers. The 2D IR experiments measure spectral diffusion, which is caused by the structural fluctuations of the bilayers. The 2D IR measurements show that the bilayer interior alkyl region dynamics occur on time scales ranging from a few picoseconds to many tens of picoseconds. These are the time scales of the bilayers' structural dynamics, which act as the dynamic solvent bath for chemical processes of membrane biomolecules. The results suggest that at least a significant fraction of the dynamics arise from density fluctuations. Samples are studied in which the cholesterol concentration is varied from 0% to 40% in both the vesicles (72 nm diameter) and fully hydrated planar bilayers in the form of aligned multibilayers. At all cholesterol concentrations, the structural dynamics are faster in the curved vesicle bilayers than in the planar bilayers. As the cholesterol concentration is increased, at a certain concentration there is a sudden change in the dynamics, that is, the dynamics abruptly slow down. However, this change occurs at a lower concentration in the vesicles (between 10% and 15% cholesterol) than in the planar bilayers (between 25% and 30% cholesterol). The sudden change in the dynamics, in addition to other IR observables, indicates a structural transition. However, the results show that the cholesterol concentration at which the transition occurs is influenced by the curvature of the bilayers.

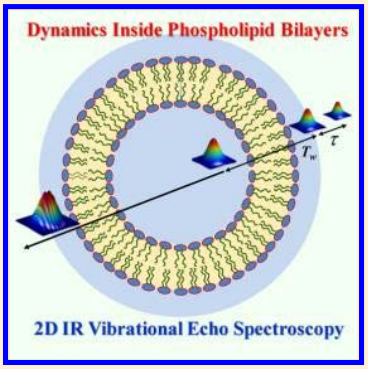

I. INTRODUCTION

Phospholipid bilayers are important models for cell membranes. Two commonly used types of bilayers are those found in vesicles[1−7] and aligned planar multibilayers.[8−14] Eukaryotic cells have sizes ranging from 10 to 30 μm. So a cell membrane has a very large radius of curvature. Eukaryotic cell membranes are much closer to planar than they are to the highly curved bilayers of vesicles. Even bacterial cells range in size from 1 to 10 μm, giving them fairly large radii of curvature. For many applications in the study of biological systems, the small radius of curvature of a vesicle probably does not matter. For example, if the model membrane is used to hold a transmembrane protein for a NMR structural study, whether the model membrane is curved or planar may make little difference.

The lipid environment of membrane bound proteins and other biomolecules influences their function,[15−19] and so impacts cell signaling, metabolism, growth, defense, and a myriad of other biological functions. While a good deal is known about the structure of artificial membranes[1,2,20−24] and orientational and translational diffusion of lipids and other molecules,[3,21,25−27] much less is known about the fast interior structural dynamics of the bilayers. In addition to other functions, cell membranes serve as the "solvent" for membrane proteins and other molecules located in membranes or that pass through membranes. Chemical processes of small molecules in solution frequently involve the solvent, which generates dynamical intermolecular interactions. For example, in many chemical reactions of small molecules or inter and intramolecular electron transfer, solvent structural fluctuations are required to bring a system to its transition state. Large biological molecules also require structural fluctuations for processes to occur. Such biomolecular motions are coupled to the solvent environment, which provides the fluctuating bath that can drive processes buried deep within a protein or enzyme.[28] For cytosolic proteins and enzymes, the solvent bath is water. Molecular dynamics (MD) simulations of cytosolic protein and enzyme dynamics use sophisticated water models that reproduce the dynamics of water's mechanical degrees of freedom. The bath degrees of freedom can be included in these MD simulations because there is a broad understanding of water dynamics, and water simulations have been tested against experiments.[29−32] The equivalent information on the ultrafast internal structural dynamics of membranes, which serve as the bath modes for membrane processes, is just beginning to emerge.[14,33]

In this Article we address the ultrafast structural dynamics as a function of cholesterol concentration of vesicle bilayers and planar bilayers in aligned multibilayers. Both types of bilayers

Special Issue: Branka M. Ladanyi Festschrift

Received: April 22, 2014
Revised: June 4, 2014
Published: June 5, 2014

dx.doi.org/10.1021/jp503940k | *J. Phys. Chem. B* 2015, 119, 8852−8862

are composed of 1,2-dilauroyl-*sn*-glycero-3-phosphocholine (dilauroylphosphatidylcholine, DLPC). Ultrafast two-dimensional infrared (2D IR) vibrational echo experiments[34−36] were used to examine the dynamics in the alkyl chain interiors of phospholipid bilayers. The experiments directly report on the time dependence of structural fluctuations of the interiors of the bilayers by measuring spectral diffusion of a vibrational probe, the antisymmetric CO stretching mode of tungsten hexacarbonyl ($W(CO)_6$). This method is very sensitive to structural changes, provides femtosecond time resolution, and can explicate the ultrafast dynamics of bilayers.

We investigate the influence of cholesterol on the dynamics because the results provide insights in the influence of the bilayer curvature on both dynamics and structure. In addition, cholesterol is an important component of many plasma membranes where it is found in concentrations that can be greater than 25%.[37] The hydroxyl group of cholesterol is hydrophilic, which results in the hydroxyl being located in the headgroup/water interfacial region. The alkyl portion of cholesterol is found in the interior alkyl regions of the bilayers. Cholesterol is known to have an impact on the structural properties of membranes. The area of phospholipids in the bilayer decreases with increasing cholesterol concentration, and the thickness of the bilayer increases.[38−40] Also, the presence of cholesterol influences the mechanical properties of membranes and the orientational order parameter.[41−43] Its presence leads to a decrease in the enthalpy of the lipid bilayer's gel to liquid-crystalline phase transition and keeps membranes in a more fluid liquid-crystalline phase.[41,44−46]

In a previous study, planar DLPC phospholipid multibilayers were studied as a function of the number of waters of hydration of the head groups and as a function of cholesterol concentration using 2D IR to measure the fast dynamics reported by the vibrational probe, $W(CO)_6$, which is also used in the current studies. The experiments showed that the head groups are fully hydrated with 16 waters of hydration. However, the cholesterol concentration study was performed on bilayers with 8 waters of hydration, that is, not fully hydrated. An increase in cholesterol concentration in partially hydrated planar lipid bilayers resulted in an abrupt slowing of the ultrafast structural dynamics in the alkyl regions with the change occurring between 30% and 35%.[14] Another study examined the structural dynamics of the interior alkyl regions of both DLPC and DPPC vesicles as a function of vesicle diameter.[33] Here we compare the influence of the concentration of cholesterol on DLPC vesicles and planar bilayers. Because the lipid head groups of vesicles are fully hydrated, the study of the influence of cholesterol on DLPC planar bilayers was repeated with fully hydrated head groups. These results, presented below, permit a direct comparison between the influence of cholesterol on vesicles and planar bilayers.

The 2D IR experimental results show that the structural dynamics of the membrane interior alkyl regions are faster in the curved bilayers of the vesicles than they are in the planar multibilayers at all cholesterol concentrations. As the concentration of cholesterol is increased, there is an abrupt decrease in the rates of structural dynamics. The sudden decrease in the rates occurs in both the planar bilayers and in the curved vesicle bilayers, indicating that both types of bilayers undergo structural as well as dynamical transitions in the interior of the membranes. However, the cholesterol concentration at which the transition occurs in the vesicles is lower (between 10% and 15%) than it is in the planar bilayers (between 25% and 30%).

II. EXPERIMENTAL PROCEDURES

A. Sample Preparation. The experiments are conducted on model membranes composed of aligned multibilayers of DLPC phospholipids.[9−14] A multibilayer is like an ordered phase of a liquid crystal. Each bilayer is planar and separated by a water layer. The samples have several thousand individual bilayers. The total sample path is 75 μm. Properly aligned bilayers provide an optically transparent medium.

Lipids were obtained from Avanti Polar Lipids, $W(CO)_6$, D_2O, and dichloromethane were purchased from Sigma-Aldrich. All chemicals were used as received. The DLPC phospholipid and the $W(CO)_6$ vibrational probe were dissolved in dichloromethane and mixed. The solvent was evaporated. For samples with cholesterol, it was also added to the solvent in the appropriate percentage prior to solvent evaporation. The cholesterol concentrations are given as the mole fraction; the sample with 10% cholesterol means there is 1 cholesterol molecule for 9 DLPC molecules. Once the solvent was evaporated, the appropriate quantity of water was added. The amount of water in the sample was verified using Karl Fischer titration.

A small amount of the phospholipid sample was placed between two CaF_2 windows with a Teflon spacer that determines the thickness. A heater and a resistance thermometer temperature probe were used to set the sample temperature for alignment and for the experiments. DLPC was aligned at 50 to 55 °C and all of the experiments discussed below were conducted at 45 °C. All planar bilayer samples contained 16 water molecules per 1 DLPC lipid molecule, which corresponds to full hydration.[14] The windows with the sample were held by a copper sample cell. The bottom of the cell was clamped to the stage of a conoscopic microscope. The top plate of the cell was very slightly loose and the plate and top window were gently slid around to produce shear that aligned the lipids into a multibilayer. The sample alignment was monitored with the microscope through crossed polarizers. The aligned regions do not rotate the light polarization and appear black. While there are bubbles and regions of unaligned lipid, large regions become aligned. It is only necessary to have aligned spots that are larger than ∼300 μm to completely pass the IR laser beams. Typically there were aligned regions of at least 1 mm and usually several millimeters. The uniformity of the aligned regions was tested.[14] $W(CO)_6$ is substantially smaller than DLPC. It has a molecular volume of ∼115 Å^3, compared to the ∼675 Å^3 molecular volume of DLPC. Concentration studies showed that at the concentrations employed (1 $W(CO)_6$ per 800 DLPC molecules) the results are independent of the $W(CO)_6$ concentration.[14] Because $W(CO)_6$ is hydrophobic, it is located mainly in the bilayer alkyl interior.[14] However, as will be discussed in greater detail below, the composition of the bilayers as well as the hydration level influences the structural properties of bilayers and the location of $W(CO)_6$.[14] At full hydration and low cholesterol concentration, some $W(CO)_6$ is found near the head groups interacting with the ester moieties of the lipids.[14] The 2D IR experiments are conducted only on the $W(CO)_6$ in the interior alkyl regions of the bilayers.

Vesicles were prepared by the extrusion method using an Avanti mini-extruder.[33] The lipid/cholesterol/$W(CO)_6$ mixture was first dissolved in dichloromethane, the dichloromethane

dx.doi.org/10.1021/jp503940k | J. Phys. Chem. B 2015, 119, 8852−8862

Table 1. FFCF Parameters (Eq 1) and Vibrational Lifetimes (T_{1a} and T_{1e}) for Fully Hydrated DLPC Planar Multibilayers with Different Amounts of Cholesterol

sample	Γ (cm^{-1})	T_2, ps	Δ_1 (cm^{-1})	τ_1 (ps)	Δ_2 (cm^{-1})	τ_2 (ps)	T_{1a} (ps)[a]	T_{1e} (ps)[a]
0%	2.9 ± 0.3	3.6 ± 0.4	1.2 ± 0.2	7.5 ± 0.8	0.9 ± 0.1	35.4 ± 2	110 ± 3	37 ± 6
10%	3.9 ± 0.3	2.6 ± 0.1	1.2 ± 0.1	9.4 ± 0.6	0.9 ± 0.1	46.3 ± 5	120 ± 6	38 ± 4
20%	3.4 ± 0.2	3.0 ± 0.2	1.4 ± 0.1	9.7 ± 0.3	0.9 ± 0.1	36.2 ± 3	117 ± 5	35 ± 3
25%	3.6 ± 0.1	2.9 ± 0.1	1.4 ± 0.1	7 ± 0.3	0.9 ± 0.1	41 ± 3	122 ± 7	32 ± 3
30%	3.6 ± 0.1	3 ± 0.2	1.4 ± 0.1	14 ± 0.4	0.8 ± 0.1	76 ± 10	137 ± 5	20 ± 2
40%	3.7 ± 0.2	2.9 ± 0.2	1.3 ± 0.1	12.5 ± 0.5	0.8 ± 0.1	71 ± 10	136 ± 9	24 ± 4

The Δ's are standard deviations. The total inhomogeneous line width is the convolution of the two Gaussian contributions, i.e., $(\Delta_1^2 + \Delta_2^2)^{1/2}$. The inhomogeneous fwhm is obtained by multiplying this number by 2.35. The total line width (fwhm) is the total inhomogeneous fwhm convolved with the homogeneous Lorentzian component fwhm, Γ. [a]T_{1a} – vibrational lifetime in alkyl region. T_{1e} – vibrational lifetime in ester region.

Table 2. FFCF Parameters (eq 1) and Vibrational Lifetimes (T_{1a} and T_{1e}) for DLPC Vesicles of 72 nm with Different Amounts of Cholesterol

sample	Γ (cm^{-1})	T_2, ps	Δ_1 (cm^{-1})	τ_1 (ps)	Δ_2 (cm^{-1})	τ_2 (ps)	T_{1a} (ps)[a]	T_{1e} (ps)[a]
0%	3.1 ± 0.3	3.4 ± 0.3	1.0 ± 0.1	4.1 ± 0.4	1.1 ± 0.1	26.4 ± 1.9	110 ± 4	36 ± 5
5%	3.2 ± 0.1	3.3 ± 0.1	0.9 ± 0.1	4 ± 0.4	1.2 ± 0.1	20.9 ± 1.2	115 ± 5	31 ± 3
10%	3.0 ± 0.2	3.5 ± 0.3	0.9 ± 0.1	3.8 ± 0.4	1.1 ± 0.1	21.7 ± 1.7	113 ± 5	32 ± 2
15%	2.8 ± 0.2	3.7 ± 0.2	1.1 ± 0.1	8.6 ± 0.9	0.9 ± 0.1	30.3 ± 3.1	123 ± 6	42 ± 5
20%	3.0 ± 0.1	3.6 ± 0.2	1.1 ± 0.1	7.4 ± 0.4	0.8 ± 0.1	36 ± 3.8	122 ± 4	43 ± 3
30%	2.9 ± 0.2	3.7 ± 0.2	1.1 ± 0.1	7.3 ± 0.6	0.9 ± 0.1	30.1 ± 2.8	122 ± 5	42 ± 4
40%	2.9 ± 0.2	3.7 ± 0.2	1 ± 0.1	6.9 ± 0.4	0.9 ± 0.1	28 ± 2	123 ± 6	40 ± 2

The Δ's are standard deviations. The total inhomogeneous line width is the convolution of the two Gaussian contributions, i.e., $(\Delta_1^2 + \Delta_2^2)^{1/2}$. The inhomogeneous fwhm is obtained by multiplying this number by 2.35. The total line width (fwhm) is the total inhomogeneous fwhm convolved with the homogeneous Lorentzian component fwhm, Γ. [a]T_{1a} – vibrational lifetime in alkyl region. T_{1e} – vibrational lifetime in ester region.

was evaporated, and the lipid was rehydrated in D_2O. The concentration of $W(CO)_6$ in the vesicle bilayers was 1 per 100 lipids. The 2D IR measurements were also made on 1 to 200 samples, which gave identical results as the 1 to 100 samples.

The lipid/cholesterol/$W(CO)_6$/D_2O solution was heated above the lipid phase transition temperature, vortexed, and extruded through a polycarbonate filtering membrane of 30 nm pore size. The vesicle size was measured by dynamic light scattering, which gave a diameter of 72 nm. The 2D IR experimental temperature was kept at 45 °C for the vesicles and the planar bilayers.

B. 2D IR and Pump–Probe Experiments. The output of a Ti:sapphire oscillator/regenerative amplifier operating at 1 kHz with a pulse energy of ~700 μJ and duration of ~100 fs was used to pump a mid-IR optical parametric amplifier (OPA). The IR pulses, which are the output of the OPA, were centered at ~1980 cm^{-1}, and had duration of 170 fs and energy of ~8 μJ/pulse.

In the 2D IR experiments,[47] the mid-infrared pulse, tuned to the peak of the absorption spectrum, was split into a weaker probe pulse and a stronger pulse. The weak pulse is routed through a mechanical delay line, which is used to set the waiting time T_w, the time between pulses 2 and 3 in the vibrational echo pulse sequence. The strong pulse was sent to a mid-infrared Fourier-domain pulse-shaper.[47] The output from the pulse shaper, which produces pulses 1 and 2 in the vibrational echo pulse sequence, was crossed in the sample with the weak probe pulse, pulse 3. After the sample, the probe is sent into a spectrograph equipped with a 32 element HgCdTe infrared array detector. The delay time between pulses 1 and 2 is τ. The vibrational echo signal is emitted following the third pulse at a time $\leq\tau$, and is also heterodyned by the third pulse.[47,48] The heterodyned vibrational echo signal is then dispersed in the spectrograph, which yields the ω_m (vertical axis) in the 2D spectrum. Scanning τ produces a time domain interferogram at each ω_m. These interferograms are Fourier transformed and yield the ω_τ (horizontal) axis of the 2D spectrum. In the experiments, τ is scanned for a fixed T_w to produce a 2D IR spectrum. T_w is then changed, and τ is again scanned to give another 2D IR spectrum. Analysis of the changes in the shape of the spectra with T_w provides the information on the structural dynamics.

As the time T_w is increased, the vibrational probe has more time to sample different structural configurations of the bilayers. Because of the bilayers' internal structure evolution, the frequency of the $W(CO)_6$ stretch changes within the distribution of frequencies reflected in the inhomogeneously broadened absorption spectrum. This frequency evolution is called spectral diffusion. Spectral diffusion is directly related to the conformational fluctuations of the membrane. The time dependence of the spectral diffusion was extracted from the 2D IR spectra using the center line slope (CLS) formalism.[49,50] The CLS method quantifies the time dependent changes in two-dimensional line shapes. The CLS is the normalized frequency–frequency correlation function (FFCF). The CLS directly gives the spectral diffusion decay times, which are caused by the time-dependent structural relaxation. The difference between the initial value of the CLS at $T_w = 0$ and 1 is related to the homogeneous component of the inhomogeneously broadened absorption line. Combining the CLS with the linear absorption spectrum allows the full FFCF to be obtained. The FFCF is the direct connection between the experimental observables and the details of the dynamics and structure of the system.

The homogeneous components and the vibrational lifetimes for planar bilayers[14] and for vesicles[33] have been discussed in detail previously. Here we are mainly interested in the decay times, as these directly reflect the times for structural relaxation.

dx.doi.org/10.1021/jp503940k | J. Phys. Chem. B 2015, 119, 8852–8862

However, there is some additional information contained in the vibrational lifetimes. As discussed below, the CLS decays are fit very well by a biexponential function.

A multiexponential form of the FFCF, $C(t)$, was used to model the FFCF.[29,49,50]

$$C(t) = \sum_{i=1}^{n} \Delta_i^2 e^{-t/\tau_i} \quad (1)$$

For the ith dynamical process, Δ_i is the range of frequencies sampled due to fluctuations of the $W(CO)_6$ environment, and τ_i is the time constant associated with these fluctuations. If $\Delta_i\tau_i < 1$, the dynamics are motionally narrowed and contribute to the homogeneous line width. The motionally narrowed dynamics are characterized by $T_2^* = 1/\Delta^2\tau$, where T_2^* is the pure dephasing time. T_2^* is the result of ultrafast structural fluctuations, typically with time scales <100 fs. The total homogeneous dephasing time, T_2, is given by $1/T_2 = 1/T_2^* + 1/2T_1 + 1/3T_{or}$. The homogeneous line width is $\Gamma = 1/\pi T_2$. T_1 is the vibrational lifetime and T_{or} is the orientational relaxation time, both of which were measured by IR pump−probe experiments.[14] All of the homogeneous dephasing line width are ~3 cm^{-1} (Tables 1 and 2). The vibrational lifetimes in the alkyl regions of the bilayers are long (~120 ps, Tables 1 and 2) and therefore contribute a negligible amount (~0.05 cm^{-1}) to the homogeneous line widths. The orientational relaxation times are all ~6 ps.[14,33] The orientational relaxation contributes ~0.6 cm^{-1} to the homogeneous line width. This is a small contribution that does not vary systematically with sample. The homogeneous line widths reported in Tables 1 and 2 contain all contributions, but are dominated by pure dephasing.

The IR pump−probe experiments are performed with the identical setup and configuration used for the 2D IR vibrational echo experiments except that the pulse shaper is programmed to give a single pulse, the pump pulse, at time $t = 0$. The probe pulse, which has horizontal polarization, is delayed using the mechanical delay line. The polarization of the pump pulse is rotated to the magic angle relative to the probe polarization using a half wave plate followed by a polarizer set at the magic angle. With the pump at the magic angle relative to the probe, only the population decay (vibrational lifetime) is measured. Orientational anisotropy decay is eliminated from the measurements. Anisotropy decay of $W(CO)_6$ in DLPC bilayer samples has been measured previously[14,33] and will be discussed further below.

III. RESULTS AND DISCUSSION

A. Absorption Spectra. Figure 1A shows the FT-IR absorption spectrum of the CO antisymmetric stretch of $W(CO)_6$ in the planar multibilayers as a function of cholesterol concentration. The bilayers are hydrated with 16 water molecules per lipid. At this water concentration, the DLPC head groups are fully hydrated.[14] The spectrum with 0% cholesterol (red curve) is the broadest of the spectra. Within experimental error it is the same as the 0% spectrum of $W(CO)_6$ in the vesicles (Figure 1B, red curve), in which the lipid head groups are fully hydrated as there is bulk water surrounding and in the interior of the vesicles.

In a previous study of $W(CO)_6$ in planar multibilayers, the absorption spectrum was studied in great detail as a function of the number of waters of hydration.[14] $W(CO)_6$ is completely insoluble in water; it resides in the interior of the bilayers. The spectra could be reproduced using the spectra of $W(CO)_6$ in

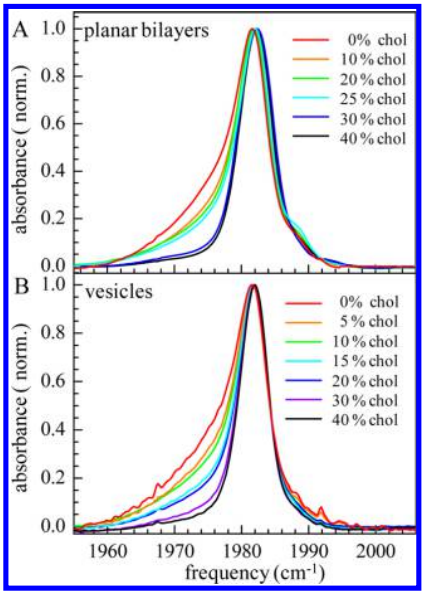

Figure 1. Background subtracted FT-IR absorption spectra of the CO antisymmetric stretching mode of $W(CO)_6$ in fully hydrated planar DLPC bilayers (A) and 72 nm DLPC vesicles (B) with different concentrations of cholesterol.

two model liquids: one was a long chain hydrocarbon, and the other was a linked diester with each ester bonded to a hydrocarbon chain (bis(2-ethylhexyl) succinate).[14,51] The studies showed that at low water concentration (2 water molecules per lipid), the spectrum was virtually identical to the spectrum of $W(CO)_6$ in the alkane. As the water concentration increased, the wing on the red (low frequency) side of the spectrum became larger in a continuous manner until it stopped changing at 16 waters of hydration. At all water concentrations, the spectrum could be reproduced as the weighted sum of $W(CO)_6$ spectra in the alkane liquid and in the diester liquid. The results showed that the $W(CO)_6$ resides in two distinct environments. It mainly resides in the alkyl region of the bilayers, which results in the narrow peak centered at 1982 cm^{-1}, but a portion of it also resides in the ester region of the phospholipid headgroup for the fully hydrated bilayers.

In Figure 1A the change in the spectrum of $W(CO)_6$ is shown as a function of cholesterol concentration. In going from 0% to 10% cholesterol, the red side wing narrows to some extent, but then it is almost identical for 10%, 20%, and 25% cholesterol concentration. At 30% cholesterol there is an abrupt change, and the wing is almost gone. The 30% and 40% spectra are virtually identical. The spectra show that adding cholesterol reduces the fraction of $W(CO)_6$ in the ester region of the bilayers, and the reduction is concentration independent to 25%. Then at 30% and higher concentrations, $W(CO)_6$ resides almost exclusively in the alkyl regions of the bilayers. As discussed below, the change in the spectra between 25% and 30% cholesterol is also the concentration change that results in a sudden slowing of the structural dynamics as well as a change in the vibrational lifetimes. In a previous study of the effect of cholesterol on the $W(CO)_6$ spectrum, planar multibilayers with 8 waters of hydration were examined.[14] These bilayers were not fully hydrated. The behavior shown in Figure 1A was also observed except the jump from spectra with a wing to spectra with virtually no wing occurred between 30% and 35%

dx.doi.org/10.1021/jp503940k | J. Phys. Chem. B 2015, 119, 8852−8862

cholesterol in 8 waters of hydration samples rather than between 25% and 30% in fully hydrated samples.

Figure 1B shows the FT-IR spectra of the antisymmetric CO stretch of $W(CO)_6$ in the vesicle bilayers as a function of cholesterol concentration. With 0% cholesterol, the spectra in the vesicle bilayers and the planar bilayers are identical within experimental error. For the vesicles, the addition of cholesterol causes the red wing to narrow, with the 5% and 10% spectra almost identical. In going from 10% to 15% there is jump reduction in the red wing. Then the 15% and 20% spectra are essentially the same. As shown below, there is a sudden change in the dynamics between 10% and 15% cholesterol. Like the planar bilayer spectra (Figure 1A), there is a sudden change in the width of the red wing with increased cholesterol concentration at the same concentration that induces the dynamical jump. However, unlike the planar bilayer spectra, for the vesicles, the 15% and 20% spectra still have a significant red wing. The red wing is effectively eliminated only when the cholesterol concentration is further increased to 30%. So the behavior of the FT-IR spectra with cholesterol concentration is different for the planar bilayers and the vesicle bilayers. This difference in the behavior may occur because of the difference in the vesicle bilayers' inner and outer leaflets.

For the planar bilayers, since the two leaflets are identical, the addition of cholesterol will have the same structural influence on both leaflets. The structural change that occurs in the planar bilayers when the cholesterol concentration reaches 30% almost eliminates the presence of $W(CO)_6$ in the ester regions of the bilayers. In the vesicle bilayers, following the initial change caused by adding 5% cholesterol, there are two clear stepwise changes in the spectrum. At 15% cholesterol the red wing is reduced, and then at 30% cholesterol, the red wing is mainly eliminated. A difference in the behavior of the two leaflets may account for the two step reduction in the red wing in the vesicle bilayers while there is a single step reduction in the planar bilayers.

B. 2D IR and Pump–Probe Experiments. Figure 2 shows 2D IR spectra of the $W(CO)_6$ antisymmetric stretch in vesicles with 10% cholesterol at short (0.3 ps) and long (100 ps) T_w. The ω_τ axis (horizontal axis) is the frequency of the first pulse in the echo sequence, which in effect labels the initial frequencies of all of the vibrational oscillators. The ω_m axis (vertical axis) is the frequency of the vibrational echo emission, which reads out the frequencies of the oscillators after the waiting time, T_w. In the upper panel, the dashed line is the diagonal. At short time, the 2D spectrum is elongated along the diagonal because the oscillator frequencies have not had time to change. The width perpendicular to the diagonal arises from the homogeneously broadened component of the spectrum. At long time, the spectrum is almost round because each initial frequency can have any final frequency within the absorption line as spectral diffusion is essentially complete (all structures have been sampled). The change in shape of the spectra with T_w, which is caused by structural evolution induced spectral diffusion, provides the dynamical information when analyzed using the CLS method.[49,50] The CLS method quantifies the change in shape of the 2D spectra with increasing T_w, and gives the time constants for the spectral diffusion. The FFCF parameters obtained from the CLS analysis are given in Tables 1 and 2. The 2D spectra and the subsequent analysis are from the $W(CO)_6$ in the alkyl regions of the FT-IR absorption spectrum (Figure 1). As discussed in detail previously,[14] the broad wing on the red side of the absorption spectrum does not contribute significantly to the 2D spectrum, and the CLS analysis is limited to the alkyl portions of the spectrum.

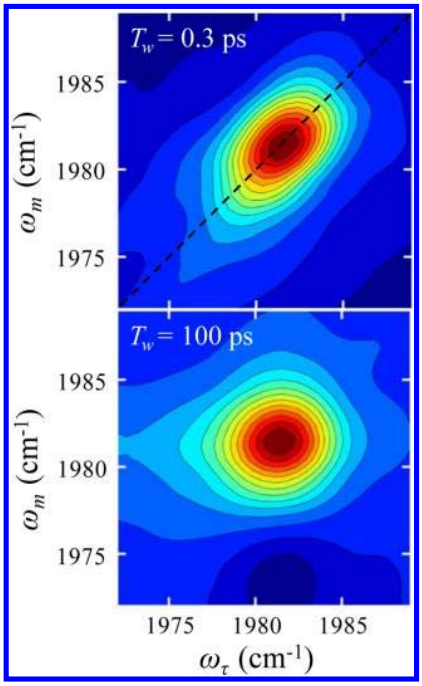

Figure 2. 2D IR vibrational echo spectra of the CO antisymmetric stretching mode of $W(CO)_6$ in 72 nm DLPC vesicle bilayers with 10% of cholesterol at short T_w = 0.3 ps, (top) and long T_w = 100 ps, (bottom). The structural dynamics of the bilayers causes the 2D line shape to change with time.

Figure 3 shows CLS decays curves (points) obtained from the 2D IR data for two cholesterol concentrations. Each point is obtained from analyzing a 2D IR spectrum at the particular T_w. The solid curves through the data are biexponential fits. As can be seen in Figure 3, in going from 10% to 30% cholesterol, both components of the decay slow down. Both components of the structural fluctuations are fast, with the 10% sample having time constants of ~4 ps and ~22 ps, and the 30% sample having time component of ~7 ps and ~30 ps. These are the times on which the vibrational probe experiences changing membrane structures in the alkyl regions of the membranes.

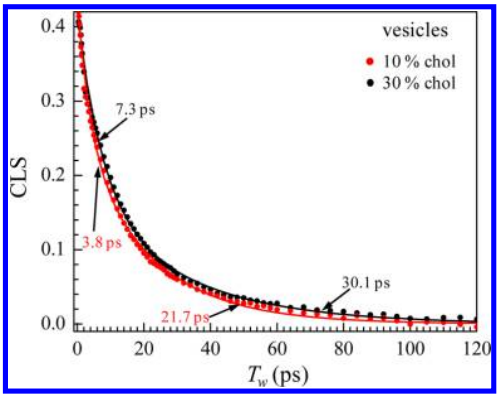

Figure 3. CLS (center line slope) decay curves obtained from the 2D IR spectra of the CO antisymmetric stretching mode of $W(CO)_6$ in 72 nm DLPC vesicle bilayers with two cholesterol concentrations (points) and biexponential fits (solid curves).

dx.doi.org/10.1021/jp503940k | J. Phys. Chem. B 2015, 119, 8852–8862

Figure 4 shows the results of the cholesterol concentration studies for planar bilayers (A) and vesicle bilayers (B). Each

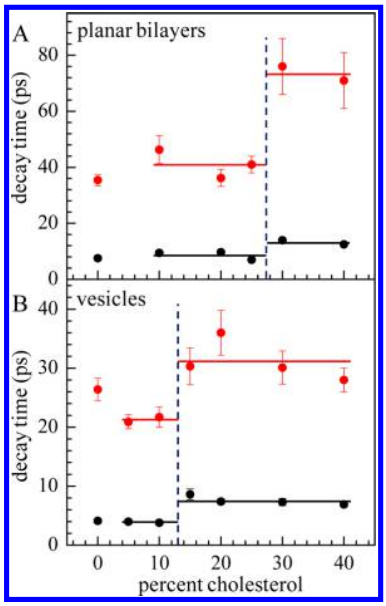

Figure 4. Fast and slow decay times obtained from the biexponential fits to the CLS decay curves for the various percent concentrations of cholesterol in fully hydrated planar DLPC bilayers (A) and 72 nm DLPC vesicles (B). The horizontal lines correspond to the average values. Tables 1 and 2 give the values of the time constants and all of the FFCF parameters.

data point is the average of the results taken on three separately prepared samples, and at least three full T_w-dependent data sets were collected on each sample. The error bars are from the combination of all of the data sets at each cholesterol concentration. Note that for the fast component, some of the error bars are smaller than the points, so they are not visible.

First consider the planar bilayer data in A. In going from 0% to 10% cholesterol, both the fast and slow components of the biexponential decay slow down. Then for 10%, 20%, and 25% cholesterol, the fast and slow components are independent of cholesterol concentration within error. However, in going from 25% to 30% (dashed line) there is a sudden change in the dynamics. Both the fast and slow components of the dynamics slow down, and the increase in the decay times is well outside of the error bars. In a previous study of DLPC planar bilayers, the cholesterol concentration was varied for samples that had eight waters of hydration per lipid.[14] These samples were not fully hydrated. The same type of behavior with cholesterol concentration was observed but with one difference. In the absence of cholesterol (0% samples), the fast and slow components are the same and independent of the number of waters of hydration.[14] However, the influence of the hydration level does matter when cholesterol is added. In the partially hydrated membranes (8 waters of hydration), the jump to slower dynamics occurred between 30% and 35% cholesterol[14] rather than between 25% and 30% observed here for the fully hydrated sample.

Now consider the behavior of the dynamics with the addition of cholesterol in the vesicle bilayers (Figure 1B; note the difference in the vertical scales between A and B). In a previous study of vesicles of different sizes with no cholesterol, the dynamics were always faster in vesicle bilayers than in planar bilayers.[33] The vesicle dynamics approached those of planar bilayers as the size of the vesicle was increased.[33] Here, regardless of the cholesterol concentration, the dynamics in the vesicle bilayers are faster than in the planar bilayers. In contrast to the planar bilayers, the first addition of cholesterol to the vesicle bilayers leaves the fast component of the dynamics unchanged and the slow component speeds up outside of the error bars. The 5% and 10% concentration samples have the same dynamics. Then between 10% and 15% cholesterol, there is an abrupt change in the dynamics. As in the planar bilayers, both components slow down. Following the jump to slower dynamics, the further addition of cholesterol does not change the time constants within the experimental error.

In Figure 1A it is seen that the spectra of the planar bilayers have three distinct manifestations as cholesterol is added. In going from 0% to 10% cholesterol, the red wing narrows. The wing then stays almost constant for 10%, 20%, and 25% cholesterol. Then at 30% cholesterol, the wing almost vanishes, and the spectrum is virtually unchanged when the cholesterol is increased to 40%. The following simple qualitative model is consistent with these observations, but certainly not proven. In addition to always being present in the alkyl regions of the bilayers, assume that the $W(CO)_6$ can reside in two types of "sites" in the ester/headgroup region of the bilayers. $W(CO)_6$ in the ester region gives rise to the red wing.[14] Now further assume that the addition of cholesterol changes the headgroup structure in a manner eliminates one of these two types of sites. Call these common sites. The cholesterol induced change in headgroup structure does not directly eliminate the other type of site, which we will call independent sites. Then the initial addition of cholesterol removes the common sites, which causes the initial decrease in the red wing. Addition of more cholesterol does not change the red wing further as the common sites are already gone, and cholesterol does not directly impact the independent site $W(CO)_6$ occupancy. However, increasing the cholesterol concentration to 30% induces an overall structural transition in the membrane. This may be the L_d (liquid disordered phase) to the L_o (liquid ordered phase) transition.[11,52−55] The structural transition eliminates the independent sites, forcing out almost all of the $W(CO)_6$ remaining in the ester region. The result is that $W(CO)_6$ is found almost entirely in the alkyl regions of the planar bilayers after the structural transition, and the red wing becomes very small. As already noted, this final large change in the spectrum occurs at the same cholesterol concentration that induces the sudden slowing of the dynamics measured with the 2D IR experiments (see Figure 4A). The simultaneous abrupt changes in the dynamics and the spectrum give substantial support to the proposition that there is a structural transition between 25% and 30% cholesterol that results in a change in the alkyl region dynamics.

There is additional information that supports a structural transition between 25% and 30% cholesterol in the planar bilayers. In the last two columns of Table 1, the vibrational lifetimes of the antisymmetric stretch of $W(CO)_6$ in the alkyl regions (T_{1a}) and in the ester regions (T_{1e}) of the bilayers are listed.[14,56] Both the T_{1a} and T_{1e} values jump in going from 25% to 30% cholesterol (see Figure 5A). The T_{1a} values slow down while the T_{1e} speed up. Vibrational lifetimes are exceedingly sensitive to the local environment. Vibrational relaxation of the high frequency stretching mode of $W(CO)_6$ will relax by exciting a combination of lower frequency intramolecular vibrations and modes of the solvent bath.[56−58] Here the solvent

dx.doi.org/10.1021/jp503940k | J. Phys. Chem. B 2015, 119, 8852−8862

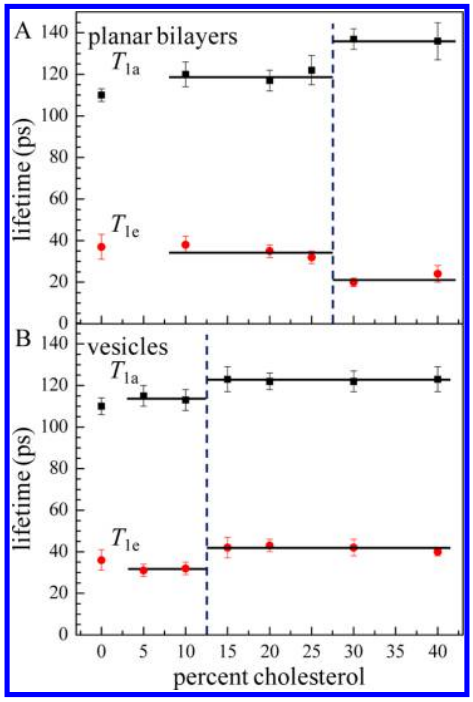

Figure 5. Vibrational lifetimes of the symmetric stretch of $W(CO)_6$ in the alkyl regions (T_{1a}) and the ester regions (T_{1e}) of the bilayers in the planar bilayers (A) and the vesicle bilayers (B). The horizontal lines are the average values.

is the membrane. Generally it is necessary to have one or more modes of the low frequency continuum of bath modes as part of the relaxation pathway to conserve energy. Changes in local structure will change the density of states of the bath modes as well as their coupling to the $W(CO)_6$ stretching mode. The fact that both lifetimes make a sudden change between 25% to 30% cholesterol shows that the structure in the alkyl regions and in the ester regions of the bilayers change at the same concentration that the spectral diffusion dynamics become slower and the vibrational spectra become narrower. Therefore, three distinct observables make an abrupt change in going from 25% to 30% cholesterol.

The same ideas discussed above can be applied to the vesicle bilayer data, but there is a difference in the behavior of the vesicle bilayers associated with the absorption spectrum. First, the planar bilayer dynamics suddenly change between 25% and 30% cholesterol while the vesicle bilayers make the jump in the spectral diffusion dynamics between 10% and 15% cholesterol. This difference demonstrates that the curvature associated with the vesicles matters.[5,6,20,21] Since the change in dynamics is most likely caused by a structural transition, these results show that a transition occurs at a cholesterol concentration that is dependent on the curvature. There have been many studies of the cholesterol induced phase transitions in vesicle bilayers.[52−54] The concentrations at which the transitions have been observed can have a dependence on the nature of the bilayer sample. Results on the cholesterol concentration in vesicles may not directly translate to the influence of cholesterol on behavior of cells where the membranes are close to planar.

The vesicle bilayers show two changes in the absorption spectrum. Between 10% and 15% cholesterol, the spectral diffusion dynamics change and the red wing in the FT-IR spectrum narrows, but, in contrast to the planar bilayers, the red wing is not reduced almost to zero. The vesicle red wing undergoes a second reduction between 25% and 30% cholesterol (see Figure 1B). There is no doubt that the red wing is caused by the presence of $W(CO)_6$ in the ester regions,[14] and, therefore, the virtual elimination of the red wing is the result of the elimination of almost all of the $W(CO)_6$ from the ester regions. It was suggested in Section III.A that this two step behavior in the spectra of the vesicles arises because the inner and outer leaflets have different structure. However, the structural dynamics transition occurs with the first red wing reduction (see Figure 4B). There is no discernible additional change in dynamics with the second reduction that almost eliminates the wing.

The question arises as to which is the major structural transition, the change at 10% to 15% demonstrated by the changes in spectral diffusion and the absorption spectrum or the further change in the absorption spectrum at 30%. The vibrational lifetimes provide further information. Both T_{1a} and T_{1e} measured in the vesicle bilayer samples (Table 2, last two columns) display stepwise changes in their values in going from 10% to15% cholesterol, and there is no further change at the 30% cholesterol level (see Figure 5B). The changes in the vibrational lifetimes, the spectral diffusion, and the absorption spectrum demonstrate that the major structural transition in the vesicle bilayers occurs between 10% and 15%.

While the structural transition in vesicle bilayers occurs in the 10% to 15% cholesterol concentration range, it is not sufficient to eliminate all of the $W(CO)_6$ from the ester regions of the bilayer. Part of the red wing remains, in contrast to planar bilayers, where the structural transition virtually eliminates the red wing. As discussed above, the difference between the vesicle bilayers and the planar bilayers in this regard may arise from the fact the inner and outer leaflets in the vesicle bilayers are not the same. One possibility is that because of the curvature of the leaflets the structural change eliminates some but not all of the common sites. Then, when the cholesterol concentration reaches a sufficiently high level in the vesicles, 30%, cholesterol occupies the independent sites, which essentially removes the red wing. This final elimination of $W(CO)_6$ from the ester region is not associated with an overall structural change as there is no corresponding change in the spectral diffusion or the vibrational lifetimes in either the alkyl regions (T_{1a}) or the ester regions (T_{1e}) as can be seen in Figures 4B and 5B.

The inhomogeneously broadening of the absorption line is caused by a variety of structural configurations of the membrane that influence the frequency of the vibrational transition of the $W(CO)_6$. Then spectral diffusion, measured with the 2D IR experiments, reports on the time evolution of these structural configurations. We can gain some insight into the nature of the structural evolution by considering the antisymmetric stretch's transition dipole anisotropy decay.[14,59] The anisotropy decay of the antisymmetric CO stretch of $W(CO)_6$ is not caused by normal molecular reorientation. The CO stretch is triply degenerate. The excitation pulse projects out a superposition of the three modes that results in the initially excited transition dipole being along the pump pulse electric field, in contrast to the usual initial cosine squared distribution of dipole directions.[59] Then fluctuations that cause the relative amplitudes of the three components of the initial superposition to change produce a change in the direction of the transition dipole without physical reorientation of the molecule.[59] Therefore, the anisotropy decay does not provide the type of information that normal orientational relaxation

dx.doi.org/10.1021/jp503940k | J. Phys. Chem. B 2015, 119, 8852−8862

measurements do and cannot be interpreted in terms of shape factors, hydrodynamic boundary conditions, or friction coefficients.

In prior work on bilayers,[14] we found that the anisotropy decay time was ~6 ps and essentially independent of the composition of the sample. This decay time is the result of the evolution of the initial superposition of degenerate modes. Consequently, on times long compared to 6 ps, the direction of the transition dipole has randomized. The fast component of the FFCF, τ_1, for the planar bilayers (Table 1) range from somewhat slower than 6 ps to more than a factor of 2 slower, while the fast component for the vesicles are somewhat faster to around 6 ps (Table 2). The dipole angular correlation function that describes the decay of the anisotropy is a different correlation function from the FFCF, so the decay times are not directly comparable. It is possible that the same fluctuations that are responsible for the fast component of FFCF are also responsible for the evolution of the degenerate mode superposition that produces the decay of the anisotropy (see below). However, the important information is that there is a significant fraction of the inhomogeneous line that is sampled on a much longer time scale. The amplitudes of the fast and slow components of the spectral diffusion, Δ_1 and Δ_2 (Tables 1 and 2), are about equal amplitude. Because the transition dipole direction randomizes on a time scale much faster than the slow component of the spectral diffusion, this slow component cannot depend on the direction of the transition dipole. Therefore, the slow component of the spectral diffusion is not caused by, for example, fluctuations of the electric field projected along the vibrational transition dipole direction, which has been invoked in a number of studies of other types of systems.[60−63] For the current system, motions of the zwitterionic headgroup as well as motions of water molecules will produce significant fluctuating electric fields. However, these motions cannot produce the longer time scale spectral diffusion or the portion of the inhomogeneous broadening reflected in Δ_2. In the alkyl region where the $W(CO)_6$ are located, the alkyl chains are virtually nonpolar, and any fluctuating electric fields they would produce would not, in any case, contribute to the long time scale spectral diffusion.

The same consideration discussed above also suggests that very local specific interactions of the lipid alkyl chains with $W(CO)_6$ are not responsible for the long time scale spectral diffusion. In the $W(CO)_6$ molecular frame, we can take the three pairs of COs to be pointing along *x*, *y*, and *z*. Each pair undergoes antisymmetric stretching. In the gas phase, these three modes would be perfectly degenerate. However, in a liquid or in the membranes under consideration here, the environment surrounding the $W(CO)_6$ will not be structurally uniform, resulting in somewhat different intermolecular interactions along *x*, *y*, and *z*. The differences will break the degeneracy and produce splittings that can contribute to the absorption line width. If local interactions do break the degeneracy, then the changes in the superposition of the bases states will cause frequency fluctuations. If such frequency fluctuations are small such that $\Delta\tau < 1$ (Δ in rad/s), these fluctuations will contribute to the homogeneous line width as pure dephasing. The time for the evolution of the superposition is the 6 ps anisotropy decay time. For the frequency fluctuations to be motionally narrowed and contribute to the pure dephasing (T_2^*), Δ must be less than ~1 cm^{-1}. In a study of $W(CO)_6$ in the hydrocarbon, 2-methylpentane, it was determined that the superposition fluctuations were motionally narrowed and contributed to the homogeneous line width.[59] If the range of energies sampled by the superposition fluctuations are large compared to 1 cm^{-1}, then these fluctuations will be observed as spectral diffusion, and they will contribute to Δ_1 in Tables 1 and 2. Because the Δ_1 values reported in the tables are all ~1 cm^{-1}, it seems more likely that the superposition fluctuations contribute to the homogeneous line width rather than to inhomogeneity and spectral diffusion. In either case, the superposition fluctuations cannot contribute to the long time scale spectral diffusion and the Δ_2 component of the inhomogeneous broadening.

Recently 2D IR spectroscopy was used to study spectral diffusion in the isotropic phase of a liquid crystal, 4-cyano-4′-pentylbiphenyl (5CB), as a function of temperature as the isotropic to nematic (I−N) phase transition was approached from above.[64,65] In the isotropic phase, the liquid has nematic order (pseudonematic domains) over a correlation length that increases as the I−N transition is approached.[66] Detailed analysis using mode coupling theory of the results of the 2D IR experiments and optical heterodyne detected optical Kerr effect experiments showed that orientational relaxation of the nematogens was far too slow to be responsible for the CN stretch spectral diffusion.[65] The spectral diffusion as well as the inhomogeneous broadening of the CN line was ascribed to density fluctuations. The density fluctuations were shown to occur on times scales consistent with the spectral diffusion, that is, a few picoseconds to a few hundred picoseconds.[65]

The bilayers studied here are substantially more ordered than the nematic order of the pseudonematic domains of 5CB. The complete orientational relaxation of the lipids is very slow, requiring the headgroup to move from one leaflet of the bilayer to the other. Based on the discussions given above, which rules out common mechanisms for spectral diffusion, it is reasonable to conclude that the slow time scale spectral diffusion, τ_2, and the corresponding contribution to the inhomogeneous broadening, Δ_2, are the result of density fluctuations as in 5CB. In 5CB it was possible to show that density fluctuations are responsible for spectral diffusion on all time scales. The same may be true here. It was argued above that the superposition state fluctuations probably contribute to homogeneous dephasing. On a time scale short compared to the anisotropy decay, fluctuations of the electric field projected along the transition dipole direction could contribute to spectral diffusion. However, looking at Tables 1 and 2, the Δ_1 values are all very similar although τ_1 ranges from 4 ps (faster than the dipole anisotropy decay) to 14 ps (significantly slower than the anisotropy decay). Δ_1 is the amplitude of the component of the inhomogeneous broadening that decays with time constant, τ_1. For times that are long compared to the anisotropy decay (6 ps), the electric field projected along the transition dipole should make at most a very small contribution to Δ_1. The same argument applies to local anisotropic interactions of $W(CO)_6$ with its environment. Therefore, it is likely that the fast component of the spectral diffusion is also caused by density fluctuations. These considerations indicate that, like 5CB, the inhomogeneous broadening of the $W(CO)_6$ absorption line and the spectral diffusion are caused by density fluctuations, and that changes with cholesterol concentrations are associated with changes in the time scales of density fluctuations.

IV. CONCLUDING REMARKS

The structural dynamics of the alkyl regions of DLPC phospholipid bilayers have been investigated as a function of

the cholesterol concentration using 2D IR vibration echo spectroscopy, vibrational lifetime measurements, and vibrational absorption spectroscopy using a vibrational probe, the antisymmetric CO stretching mode of $W(CO)_6$. The results for fully hydrated planar bilayers in multibilayer samples were compared to the results for vesicle bilayers (72 nm diameter). The 2D IR experiments measure spectral diffusion. The data were analyzed for $W(CO)_6$ located in the alkyl regions of the bilayers. Spectral diffusion is caused by the structural fluctuations of the bilayers, most likely density fluctuations. The structural fluctuations occur on several time scales from a few picoseconds to many tens of picoseconds. For all cholesterol concentrations, including 0%, the structural dynamics are slower in the planar bilayers than in the vesicle bilayers. As shown in Figure 4, in both the planar bilayers and in the vesicle bilayers, as the cholesterol concentration is increased, the dynamics make a sudden jump to slower dynamics. However, the jump in the planar bilayers occurs between 25% and 30% cholesterol while the jump occurs between 10% and 15% in the vesicle bilayers.

In addition to the 2D IR experiments, two other observables were investigated as a function of concentration, the absorption spectra (Figure 1) and the vibrational lifetimes (Figure 5) of the antisymmetric CO stretch of $W(CO)_6$. Both the spectra and the vibrational lifetimes show discontinuous behavior at the same concentrations at which the 2D IR data makes an abrupt jump. Both the vibrational spectra and the lifetimes are sensitive to the local environments of the $W(CO)_6$. The fact that three different observables jump to new values at the same cholesterol concentrations strongly supports the proposition that these changes are induced by a structural transition in the membranes. This structural change is likely to be the L_d to L_o transition. An important difference between the planar bilayers and the vesicle bilayers is the fact that the structural transitions occur at different cholesterol concentrations. Therefore, consideration of the influence of cholesterol concentration on phospholipid bilayer structure needs to take into account the curvature of the bilayer system under study.

In both planar and vesicle bilayers, the structural fluctuations of the alkyl region are very fast. For transmembrane proteins and other membrane bound biomolecules, these structural fluctuations are the equivalent of the solvent structural fluctuations experienced by a solute in a liquid solvent. The phase transition with sufficient cholesterol changes the time constants of the membrane structural fluctuations. Fluctuations of membranes will be coupled to the dynamics of proteins and other membrane molecules and can play a role in their structural dynamics and therefore the function of molecules that reside in or span the alkyl regions of membranes.

AUTHOR INFORMATION

Corresponding Author

*E-mail: fayer@stanford.edu.

Notes

The authors declare no competing financial interest.

ACKNOWLEDGMENTS

This work was funded by the Division of Chemical Sciences, Geosciences, and Biosciences, Office of Basic Energy Sciences of the U.S. Department of Energy through Grant # DE-FG03-84ER13251 and by the Division of Chemistry, Directorate of Mathematical and Physical Sciences, National Science Foundation Grant # CHE-1157772 for partial support of the personnel and instrumentation used in these experiments. A.T. thanks the Stanford Graduate Fellowship program for a research fellowship.

REFERENCES

(1) Kiselev, M. A.; Zemlyanaya, E. V.; Aswal, V. K.; Neubert, R. H. H. What Can We Learn About the Lipid Vesicle Structure from the Small-Angle Neutron Scattering Experiment? *Eur. Biophys J. Biophys.* **2006**, *35*, 477−493.

(2) Schmiedel, H.; Almasy, L.; Klose, G. Multilamellarity, Structure and Hydration of Extruded POPC Vesicles by SANS. *Eur. Biophys. J. Biophys.* **2006**, *35*, 181−189.

(3) Zhu, T.; Jiang, Z. Y.; Ma, Y. Q. Lipid Exchange between Membranes: Effects of Membrane Surface Charge, Composition, and Curvature. *Colloid Surf. B* **2012**, *97*, 155−161.

(4) Yokoyama, H.; Ikeda, K.; Wakabayashi, M.; Ishihama, Y.; Nakano, M. Effects of Lipid Membrane Curvature on Lipid Packing State Evaluated by Isothermal Titration Calorimetry. *Langmuir* **2013**, *29*, 857−860.

(5) Nir, S.; Wilschut, J.; Bentz, J. The Rate of Fusion of Phospholipid-Vesicles and the Role of Bilayer Curvature. *Biochim. Biophys. Acta* **1982**, *688*, 275−278.

(6) Ahmed, S.; Wunder, S. L. Effect of High Surface Curvature on the Main Phase Transition of Supported Phospholipid Bilayers on SiO_2 Nanoparticles. *Langmuir* **2009**, *25*, 3682−3691.

(7) Rutkowski, C. A.; Williams, L. M.; Haines, T. H.; Cummins, H. Z. The Elasticity of Synthetic Phospholipid-Vesicles Obtained by Photon-Correlation Spectroscopy. *Biochemistry* **1991**, *30*, 5688−5696.

(8) Asher, S. A.; Pershan, P. S. Alignment and Defect Structures in Oriented Phosphatidylcholine Multilayers. *Biophys. J.* **1979**, *27*, 393−422.

(9) Zhao, W.; Moilanen, D. E.; Fenn, E. E.; Fayer, M. D. Water at the Surfaces of Aligned Phospholipid Multi-Bilayer Model Membranes Probed with Ultrafast Vibrational Spectroscopy. *J. Am. Chem. Soc.* **2008**, *130*, 13927−13937.

(10) Metzler, D. E. *Biochemistry: The Chemical Reactions of Living Cells*; 2nd ed.; Harcourt/Academic Press: San Diego, 2001.

(11) Nagle, J. F.; Tristram-Nagle, S. Structure of Lipid Bilayers. *Biochim. Biophys. Acta: Rev. Biomembr.* **2000**, *1469*, 159−195.

(12) Tristram-Nagle, S.; Nagle, J. F. Lipid Bilayers: Thermodynamics, Structure, Fluctuations, and Interactions. *Chem. Phys. Lipids* **2004**, *127*, 3−14.

(13) Milhaud, J. New Insights into Water−Phospholipid Model Membrane Interactions. *Biochim. Biophys. Acta* **2004**, *1663*, 19−51.

(14) Kel, O.; Tamimi, A.; Thielges, M. C.; Fayer, M. D. Ultrafast Structural Dynamics inside Planar Phospholipid Multibilayer Model Cell Membranes Measured with 2D IR Spectroscopy. *J. Am. Chem. Soc.* **2013**, *135*, 11063−11074.

(15) Janmey, P. A.; Kinnunen, P. K. J. Biophysical Properties of Lipids and Dynamic Membranes. *Trends Cell Biol.* **2006**, *16*, 538−546.

(16) Lee, A. G. How Lipids Affect the Activities of Integral Membrane Proteins. *Biochim. Biophys. Acta* **2004**, *1666*, 62−87.

(17) Mcintosh, T. J.; Simon, S. A. Roles of Bilayer Material Properties in Function and Distribution of Membrane Proteins. *Annu. Rev. Biophys. Biomol. Struct.* **2006**, *35*, 177−198.

(18) Jensen, M. O.; Mouritsen, O. G. Lipids Do Influence Protein Function - The Hydrophobic Matching Hypothesis Revisited. *Biochim. Biophys. Acta: Biomembranes* **2004**, *1666*, 205−226.

(19) Bienveniie, M.; Marie, J. S. Modulation of Protein Function by Lipids. *Curr. Top. Membr.* **1994**, *40*, 319−354.

(20) Kucerka, N.; Pencer, J.; Sachs, J. N.; Nagle, J. F.; Katsaras, J. Curvature Effect on the Structure of Phospholipid Bilayers. *Langmuir* **2007**, *23*, 1292−1299.

(21) Risselada, H. J.; Marrink, S. J. Curvature Effects on Lipid Packing and Dynamics in Liposomes Revealed by Coarse Grained Molecular Dynamics Simulations. *Phys. Chem. Chem. Phys.* **2009**, *11*, 2056−2067.

(22) Lin, C. M.; Li, C. S.; Sheng, Y. J.; Wu, D. T.; Tsao, H. K. Size-Dependent Properties of Small Unilamellar Vesicles Formed by Model Lipids. *Langmuir* **2012**, *28*, 689−700.
(23) Huang, C.; Mason, J. T. Geometric Packing Constraints in Egg Phosphatidylcholine Vesicles. *Proc. Nat. Acad. Sci. U.S.A.* **1978**, *75*, 308−310.
(24) Brzustowicz, M. R.; Brunger, A. T. X-ray Scattering from Unilamellar Lipid Vesicles. *J. Appl. Crystallogr.* **2005**, *38*, 126−131.
(25) Shintani, M.; Yoshida, K.; Sakuraba, S.; Nakahara, M.; Matubayasi, N. NMR-NOE and MD Simulation Study on Phospholipid Membranes: Dependence on Membrane Diameter and Multiple Time Scale Dynamics. *J. Phys. Chem. B* **2011**, *115*, 9106−9115.
(26) Bocian, D. F.; Chan, S. I. NMR-Studies of Membrane Structure and Dynamics. *Annu. Rev. Phys. Chem.* **1978**, *29*, 307−335.
(27) Parmar, Y. I.; Wassall, S. R.; Cushley, R. J. Orientational Order in Phospholipid-Bilayers − ^{2}H NMR-Study of Selectively Deuterated Palmitic Acids in Unilamellar Vesicles. *J. Am. Chem. Soc.* **1984**, *106*, 2434−2435.
(28) Thielges, M. C.; Chung, J. K.; Fayer, M. D. Protein Dynamics in Cytochrome P450 Molecular Recognition and Substrate Specificity Using 2D IR Vibrational Echo Spectroscopy. *J. Am. Chem. Soc.* **2010**, *133*, 3995−4004.
(29) Asbury, J. B.; Steinel, T.; Kwak, K.; Corcelli, S. A.; Lawrence, C. P.; Skinner, J. L.; Fayer, M. D. Dynamics of Water Probed with Vibrational Echo Correlation Spectroscopy. *J. Chem. Phys.* **2004**, *121*, 12431−12446.
(30) Asbury, J. B.; Steinel, T.; Stromberg, C.; Corcelli, S. A.; Lawrence, C. P.; Skinner, J. L.; Fayer, M. D. Water Dynamics: Vibrational Echo Correlation Spectroscopy and Comparison to Molecular Dynamics Simulations. *J. Phys.Chem. A* **2004**, *108*, 1107−1119.
(31) Fecko, C. J.; Loparo, J. J.; Roberts, S. T.; Tokmakoff, A. Local Hydrogen Bonding Dynamics and Collective Reorganization in Water: Ultrafast Infrared Spectroscopy of HOD/D_2O. *J. Chem. Phys.* **2005**, *122*, 054506.
(32) Fecko, C. J.; Eaves, J. D.; Loparo, J. J.; Tokmakoff, A.; Geissler, P. L. Local and Collective Hydrogen Bond Dynamics in the Ultrafast Vibrational Spectroscopy of Liquid Water. *Science* **2003**, *301*, 1698−1702.
(33) Kel, O.; Tamimi, A.; Fayer, M. D. Size Dependent Ultrafast Structural Dynamics inside Phospholipid Vesicle Bilayers Measured with 2D IR Vibrational Echo Spectroscopy. *Proc. Nat. Acad. Sci. U.S.A.* **2014**, *111*, 918−923.
(34) Park, S.; Kwak, K.; Fayer, M. D. Ultrafast 2D-IR Vibrational Echo Spectroscopy: A Probe of Molecular Dynamics. *Laser Phys. Lett.* **2007**, *4*, 704−718.
(35) Zheng, J.; Kwak, K.; Fayer, M. D. Ultrafast 2D IR Vibrational Echo Spectroscopy. *Acc. Chem. Res.* **2007**, *40*, 75−83.
(36) Thielges, M. C.; Fayer, M. D. Protein Dynamics Studied with Ultrafast 2D IR Vibrational Echo Spectroscopy. *Acc. Chem. Res.* **2012**, *45*, 1866−1874.
(37) McIntosh, T. J. Structue and Physical Properties of the Lipid Membrane. *Cur. Top. Membranes* **1999**, *38*, 23−47.
(38) Lecuyer, H.; Dervichian, D. G. Structure of Aqueous Mixtures of Lecithin and Cholesterol. *J. Mol. Biol.* **1969**, *45*, 39−57.
(39) Pan, J.; Mills, T. T.; Tristram-Nagle, S.; Nagle, J. F. Cholesterol Perturbs Lipid Bilayers Nonuniversally. *Phys. Rev. Lett.* **2008**, *100*, 198103.
(40) Pan, J.; Tristram-Nagle, S.; Nagle, J. F. Effect of Cholesterol on Structural and Mechanical Properties of Membranes Depends on Lipid Chain Saturation. *Phys. Rev. E* **2009**, *80*, 021931.
(41) El-Sayed, M. Y.; Guion, T. A.; Fayer, M. D. Effect of Cholesterol on Viscoelastic Properties of Dipalmitoylphosphatidyl Choline Multibilayers, as Measured by a Laser Induced Ultrasonic Probe. *Biochemistry* **1986**, *25*, 4825−4832.
(42) Martinez, G. V.; Dykstra, E. M.; Lope-Piedrafita, S.; Job, C.; Brown, M. F. NMR Elastometry of Fluid Membranes in the Mesoscopic Regime. *Phys. Rev. E* **2002**, *66*, 050902.
(43) Hsieh, C. J.; Chen, Y. W.; Hwang, D. W. Effects of Cholesterol on Membrane Molecular Dynamics Studied by Fast Field Cycling NMR Relaxometry. *Phys. Chem. Chem. Phys.* **2013**, *15*, 16634.
(44) Ladbrook, B. D.; Williams, R. M.; Chapman, D. Studies on Lecithin−Cholesterol−Water Interactions by Differential Scanning Calorimetry and X-ray Diffraction. *Biochim. Biophys. Acta* **1968**, *150*, 333−340.
(45) Calhoun, W. I.; Shipley, G. G. Sphingomyelin−Lecithin Bilayers and Their Interaction with Cholesterol. *Biochemistry* **1979**, *18*, 1717−1722.
(46) Needham, D.; Nunn, R. S. Elastic-Deformation and Failure of Lipid Bilayer-Membranes Containing Cholesterol. *Biophys. J.* **1990**, *58*, 997−1009.
(47) Kumar, K. S. K.; Tamimi, A.; Fayer, M. D. Comparisons of 2D IR Measured Spectral Diffusion in Rotating Frames Using Pulse Shaping and in the Stationary Frame Using the Standard Method. *J. Chem. Phys.* **2012**, *137*, 184201.
(48) Shim, S.-H.; Zanni, M. T. How to Turn Your Pump−Probe Instrument into a Multidimensional Spectrometer: 2D IR and Vis Spectroscopies via Pulse Shaping. *Phys. Chem. Chem. Phys.* **2009**, *11*, 748−761.
(49) Kwak, K.; Park, S.; Finkelstein, I. J.; Fayer, M. D. Frequency−Frequency Correlation Functions and Apodization in 2D-IR Vibrational Echo Spectroscopy, a New Approach. *J. Chem. Phys.* **2007**, *127*, 124503.
(50) Kwak, K.; Rosenfeld, D. E.; Fayer, M. D. Taking Apart 2D-IR Vibrational Echo Spectra: More Information and Elimination of Distortions. *J. Chem. Phys.* **2008**, *128*, 204505.
(51) Kumar, K. S. K.; Tamimi, A.; Fayer, M. D. Dynamics in the Interior of AOT Lamellae Investigated with 2D IR Spectroscopy. *J. Am. Chem. Soc.* **2013**, *135*, 5118−5126.
(52) Chiang, Y. W.; Costa, A. J.; Freed, J. H. Dynamic Molecular Structure and Phase Diagram of DPPC-Cholesterol Binary Mixtures: A 2D-ELDOR Study. *J. Phys. Chem. B* **2007**, *111*, 11260−11270.
(53) Vist, M. R.; Davis, J. H. Phase-Equilibria of Cholesterol Dipalmitoylphosphatidylcholine Mixtures: ^{2}H Nuclear Magnetic-Resonance and Differential Scanning Calorimetry. *Biochemistry* **1990**, *29*, 451−464.
(54) Tenchov, B. G. Nonuniform Lipid Distribution in Membranes. *Prog. Surf. Sci.* **1985**, *20*, 273−340.
(55) Koynova, R.; Caffrey, M. An Index of Lipid Phase Diagrams. *Chem. and Phys. of Lipids* **2002**, *115*, 107−219.
(56) Kenkre, V. M.; Tokmakoff, A.; Fayer, M. D. Theory of Vibrational Relaxation of Polyatomic Molecules in Liquids. *J. Chem. Phys.* **1994**, *101*, 10618.
(57) Keyes, T. Instantaneous Normal Mode Approach to Liquid State Dynamics. *J. Phys. Chem. A* **1997**, *101*, 2921.
(58) Tokmakoff, A.; Sauter, B.; Fayer, M. D. Temperature-Dependent Vibrational Relaxation in Polyatomic Liquids: Picosecond Infrared Pump−Probe Experiments. *J. Chem. Phys.* **1994**, *100*, 9035−9043.
(59) Tokmakoff, A.; Urdahl, R. S.; Zimdars, D.; Francis, R. S.; Kwok, S.; Fayer, M. D. Vibrational Spectral Diffusion and Population Dynamics in a Glass-Forming Liquid: Variable Bandwidth Picosecond Infrared Spectroscopy. *J. Chem. Phys.* **1995**, *102*, 3919−3931.
(60) Eaves, J. D.; Tokmakoff, A.; Geissler, P. L. Electric Field Fluctuations Drive Vibrational Dephasing in Water. *J. Phys. Chem. A* **2005**, *109*, 9424−9436.
(61) Williams, R. B.; Loring, R. F.; Fayer, M. D. Vibrational Dephasing of Carbonmonoxy Myoglobin. *J. Phys. Chem. B* **2001**, *105*, 4068−4071.
(62) Bagchi, S.; Nebgen, B. T.; Loring, R. F.; Fayer, M. D. Dynamics of a Myoglobin Mutant Enzyme: 2D-IR Vibrational Echo Experiments and Simulations. *J. Am. Chem. Soc.* **2010**, *132*, 18367−18376.
(63) Bagchi, S.; Boxer, S. G.; Fayer, M. D.; Ribonuclease, S. Dynamics Measured Using a Nitrile Label with 2D IR Vibrational Echo Spectroscopy. *J. Phys. Chem. B* **2012**, *116*, 4034−4042.
(64) Sokolowsky, K. P.; Fayer, M. D. Dynamics in the Isotropic Phase of Nematogens Using 2D IR Vibrational Echo Measurements

on Natural Abundance ^{13}CN and Extended Lifetime Probes. *J. Phys. Chem. B* **2013**, *117*, 15060−15071.
(65) Sokolowsky, K. P.; Bailey, H. E.; Fayer, M. D. Length Scales and Structural Dynamics in Nematogen Pseudonematic Domains Measured with 2D IR Vibrational Echoes and Optical Kerr Effect Experiments. *J. Phys. Chem. B* **2014**, DOI: 10.1021/jp500144p.
(66) deGennes, P. G. *The Physics of Liquid Crystals*; Clarendon Press: Oxford, 1974.